

Mutational landscape of high-grade B-cell lymphoma with *MYC*-, *BCL2* and/or *BCL6* rearrangements characterized by whole-exome sequencing

Axel Kunstner,^{1,2,3*} Hanno M. Witte,^{4,5*} Jörg Riedl,^{4,6*} Veronica Bernard,⁶ Stephanie Stölting,⁶ Hartmut Merz,⁶ Vito Olschewski,⁴ Wolfgang Peter,^{7,8} Julius Ketzner,⁹ Yannik Busch,⁷ Peter Trojok,⁷ Nikolas von Bubnoff,^{3,4} Hauke Busch,^{1,2,3#} Alfred C. Feller^{6#} and Niklas Gebauer^{3,4#}

¹Medical Systems Biology Group, University of Lübeck, Lübeck; ²Institute for Cardiogenetics, University of Lübeck, Lübeck; ³University Cancer Center Schleswig-Holstein, University Hospital of Schleswig-Holstein, Campus Lübeck, Lübeck; ⁴Department of Hematology and Oncology, University Hospital of Schleswig-Holstein, Campus Lübeck, Lübeck; ⁵Department of Hematology and Oncology, Federal Armed Forces Hospital Ulm, Ulm; ⁶Hämatopathologie Lübeck, Reference Center for Lymph Node Pathology and Hematopathology, Lübeck; ⁷HLA Typing Laboratory of the Stefan-Morsch-Foundation; ⁸University of Cologne, Faculty of Medicine and University Hospital Cologne, Institute for Transfusion Medicine, Cologne and ⁹Department of Pediatrics, University Hospital of Schleswig-Holstein, Campus Lübeck, Lübeck, Germany

*AK, HMW and JR contributed equally as co-first authors.

#HB, ACF and NG contributed equally as co-senior authors.

Correspondence:

Niklas Gebauer
Niklas.Gebauer@uksh.de

Received: July 15, 2021.


Accepted: November 9, 2021.

Prepublished: November 18, 2021.

<https://doi.org/10.3324/haematol.2021.279631>

©2022 Ferrata Storti Foundation

Haematologica material is published under

a CC-BY-NC license 

Abstract

High-grade B-cell lymphoma accompanied with double/triple-hit *MYC* and *BCL2* and/or *BCL6* rearrangements (HGBL-DH/TH) poses a cytogenetically-defined provisional entity among aggressive B-cell lymphomas that is traditionally associated with unfavorable prognosis. In order to better understand the mutational and molecular landscape of HGBL-DH/TH we here performed whole-exome sequencing and deep panel next-generation sequencing of 47 clinically annotated cases. Oncogenic drivers, mutational signatures and perturbed pathways were compared with data from follicular lymphoma (FL), diffuse large B-cell lymphoma (DLBCL) and Burkitt lymphoma (BL). We find an accumulation of oncogenic mutations in NOTCH, IL6/JAK/STAT and NFκB signaling pathways and delineate the mutational relationship within the continuum between FL/DLBCL, HGBL-DH/TH and BL. Further, we provide evidence of a molecular divergence between *BCL2* and *BCL6* rearranged HGBL-DH. Beyond a significant congruency with the C3/EZB DLBCL cluster in *BCL2* rearranged cases on an exome-wide level, we observe an enrichment of the SBS6 mutation signature in *BCL6* rearranged cases. Differential gene set enrichment and subsequent network propagation analysis according to cytogenetically defined subgroups revealed an impairment of *TP53* and *MYC* pathway signaling in *BCL2* rearranged cases, whereas *BCL6* rearranged cases lacked this enrichment, but instead showed impairment of E2F targets. Intriguingly, HGBL-TH displayed intermediate mutational features considering all three aspects. This study elucidates a recurrent pattern of mutational events driving FL into *MYC*-driven *BCL2*-rearranged HGBL, unveiling the mutational pathogenesis of this provisional entity. Through this refinement of the molecular taxonomy for aggressive, germinal center-derived B-cell lymphomas, this calls into question the current World Health Organization classification system, especially regarding the status of *MYC/BCL6*-rearranged HGBL.

Introduction

High-grade B-cell lymphoma (HGBL) with *MYC*-, *BCL2* and/or *BCL6* rearrangements poses a novel, yet provisional, cytogenetically-defined entity within the current World Health Organization classification of lymphoid tumors. It is allocated in the pathobiological continuum be-

tween diffuse large B-cell (DLBCL) and Burkitt lymphoma (BL).¹ The t(8;14)(q24;q32) IgH/*MYC* rearrangement constitutes the molecular hallmark of BL. This or further derivative chromosomal rearrangements that juxtapose *MYC* to a genomic enhancer, occur in approximately 10% of DLBCL and have been shown to correlate with inferior clinical outcome.² The rearrangement is a driver of oncogenesis

that is accompanied in approximately 50% of cases by additional rearrangements involving *BCL2* and/or *BCL6* and referred to as double-hit (DH) or triple-hit (TH) lymphomas.³⁻¹¹

While the clinical outcome in double/triple-hit HGBL (HGBL-DH/TH) patients is generally poor, recent studies have hinted at a significant impact of *MYC* translocation partners and defined *MYC/Ig* rearrangements to be the most reliable predictors of adverse outcome.^{2,7}

In a prior study, we discovered an elevated frequency of *TP53* impairment in *MYC*-driven DH/TH, whose presence was subsequently demonstrated for a subset of patients with a single-hit *MYC* translocation as well, indicating inferior outcome.^{12,13}

By conventional cytogenetics HGBL-DH/TH were shown to recurrently harbor a complex karyotype.⁴ Data on the genetic basis of this entity, however, remains elusive. Several preliminary studies, predominantly focusing on HGBL-DH/TH with DLBCL morphology, have employed a panel-based next-generation sequencing (NGS) approach.¹⁴⁻¹⁶ The insights from these studies were all restricted by gene panel design and the associated clinicopathological data, even though their central assertions included a significant enrichment in mutations affecting *CREBBP*, *BCL2* and *KMT2D* alongside an overall reflection of the phenotypical gray zone between DLBCL and BL. Most recently, Cucco et al. elucidated significant aspects of the molecular signature of HGBL in a panel-based sequencing and gene expression study, employing a 70-gene HaloPlex panel and an array-based gene expression approach. The authors restricted their study to samples with DLBCL morphology that stemmed from a clinical trial and the UK's population-based Hematological Malignancy Research Network.¹⁷

A comprehensive, exome-wide assessment of oncogenic driver mutations in HGBL-DH/TH, including cases with BL-like morphology is, however, still warranted and of vital importance to the refinement of the pathogenetic understanding of this clinically challenging entity ultimately enabling targeted therapeutic approaches.

We therefore conducted a whole-exome sequencing (WES) study on a large cohort of HGBL-DH/TH, validated by panel-based NGS and supplemented these data with a comprehensive clinicopathological assessment of the study group. Here, we report on oncogenic drivers, somatic copy number alterations (SCNA) and putative pathway perturbations, thus refining the molecular taxonomy of *MYC*-driven germinal center-derived aggressive lymphomas.

Methods

Case selection and clinicopathological characteristics

In a retrospective approach, we reviewed our institutional database to identify HGBL patients whose primary diag-

nostic biopsy specimen had been referred to the Reference Center for Hematopathology, University Hospital Schleswig Holstein, Campus Lübeck and Hämatopathologie Lübeck for centralized histopathological panel evaluation between January 2007 and December 2019. For additional Information on clinicopathological work-up, please see the *Online Supplementary Appendix* and the *Online Supplementary Table S1*.

This retrospective study was approved by the ethics committee of the University of Lübeck (reference number 18-356) and conducted in accordance with the Declaration of Helsinki. Patients had given written informed consent regarding routine diagnostic and academic assessment of their biopsy specimen including molecular studies at the Reference Center for Hematopathology and transfer of their clinical data.

Whole-exome and targeted amplicon-based sequencing

WES of n=47 HGBL-DH/TH samples was performed by a hybrid capture approach with the Agilent SureSelect Human All Exon V6 library preparation kit (Agilent Technologies) followed by Illumina short read sequencing on a NovaSeq platform (Illumina) to an average depth of 304x (standard deviation $\pm 195x$; median 234x; sequencing depth was estimated using *mosdepth* v0.3.2)¹⁸ by Novogene (UK) Co., Ltd (*Online Supplementary Table S2*). Seeking to validate the initial delineation of the exome sequencing-derived mutational landscape in HGBL we employed our in-house custom AmpliSeq panel (Thermo Fisher Scientific, Waltham, MA, USA) for targeted amplicon sequencing (tNGS), encompassing all coding exons of 43 genes (see *Online Supplementary Table S3*) in 21 cases. DNA preparation for validation experiments was extracted from the same sample but in an independent approach from deeper tissue sections. Raw paired-end data (*fastq* format) was trimmed and quality filtered using *FASTP* (v0.20.0; minimum length 50 bp, maximum unqualified bases 30%, trim tail set to 1)¹⁹ and trimmed reads were mapped to GRCh37/hg19 using *BWA MEM* (v0.7.15).²⁰ Resulting alignment files in *SAM* format were cleaned, sorted, and converted into *BAM* format using *PICARD TOOLS* (v2.18.4). Single nucleotide variants (SNV), as well as short insertions and deletions (InDels) were identified following the best practices for somatic mutations calling provided by *GATK*.²¹ Somatic copy number aberrations (SCNA) were identified by *CONTROL-FREEC* (v11.4).²² For further details on nucleic acid extraction, panel sequencing, single nucleotide and copy number variant calling please see the *Online Supplementary Appendix*.

Mutational deleteriousness and significance, network propagation, gene set enrichment and mutational cluster analysis

The MUTSIGCV algorithm was employed on WES data to

delineate significantly mutated genes within the study cohort while deleteriousness was assessed via the CADD v1.3. The acquired genomic data were then processed through the LymphGen algorithm and underwent manual screening for an enrichment in overlapping aberrations with the molecular clusters proposed by Chapuy *et al.* followed by validation through a logistic regression framework.^{23,24} Cytogenetically defined subgroups (HGBL with *MYC* and *BCL2* aberrations, HGBL with *MYC* and *BCL6* aberrations, and HGBL-TH) underwent differential downstream analysis by a network propagation approach simulating a protein-protein interaction network. Subsequently gene set variation analysis was performed against HALLMARK gene sets.

For details including statistical approaches correlating molecular and clinicopathological findings please see the *Online Supplementary Appendix*.

Results

Clinicopathological characteristics of the study group

We collected 47 cases of HGBL-DH/TH at diagnosis with sufficient formalin-fixed, paraffin-embedded (FFPE) tissue samples for molecular studies (median age 71 years; range, 35–89 years) all of which were included in the final analysis, following successful library preparation for WES. There was insufficient clinical follow-up in nine of 47 (19%) cases. An underlying HIV infection was clinically excluded in all cases. The majority of patients in our study were male (25/47; 53%) and presented with advanced stage disease (24/38 stage III/IV; 63%) and an adverse prognostic constellation (24/38 [63%], revised International Prognostic Index [R-IPI] >2). Most patients received an intensive cyclophosphamide, doxorubicin hydrochloride, vincristine sulfate, and prednisone (CHOP)-like therapeutic frontline approach (25/38; 66%). The overall response rate after first line (immuno-) chemotherapy was 76% resembling a general therapeutic response in 29 of 38 cases.

Table 1 summarizes the baseline characteristics of all HGBL-DH/TH cases included in the current study. Histologically, the predominant morphology was that of DLBCL (NOS) (32/47), however, Burkitt-like morphology and immunophenotype was present in 15 of 47 patients. Cytogenetically 21 of 47 cases presented with *MYC/BCL2*, 17 of 47 presented with *MYC/BCL6* DH constellation and nine TH lymphomas were included. *MYC* translocation partner revealed *MYC*-Ig rearrangement in eight of 17 cases. The treatment outcome in our cohort was unfavorable yet in keeping with previous data reported by Rosenwald and colleagues.² For confirmatory purposes, we included four cases, which were assessed for *TP53* mutation status in a previous study and were able to validate both cytogenetic

as well as molecular observations.¹²

The mutational landscape of double-/triple-hit high-grade B-cell lymphoma identified by whole-exome sequencing

In order to characterize the mutational landscape in an extensive cohort of HGBL-DH/TH cases, we successfully performed WES in 47 patient-derived tumor biopsies and matched constitutional DNA in seven cases. We further applied the analytical framework outlined above to analyze WES data in the absence of paired germline DNA in the majority of cases. Following the primary identification of SNV and Indels in individual samples and subsequent filtering to correct for FFPE-derived artefacts and spurious mutations, we applied the MutSig2CV algorithm and thereby identified 22 significant candidate driver genes ($P < 0.001$; 13 genes with $q < 0.1$; *Online Supplementary Table S4*).²⁵

All HGBL-DH/TH cases carried mutations in genes of oncogenic relevance according to our bioinformatic annotations. In total, we described 10,092 presumably harmful somatic mutations (cut-off see materials and methods) involving 5,521 genes after variant filtering. Of these, SNV and Indels represented 74.1% of the mutations (7,479 SNV). Among them, missense mutations were the most frequent alterations (85.2%), followed by nonsense (5.7%) and Indels (5.6%), while splice site mutations posed 3.3% of somatic mutations (Figure 1A). Displaying an overall intermediate tumor mutational burden (median 3.974; range, 1.065–18.234 mutations/Mbase; Figure 1B), HGBL-DH/TH revealed no evidence of MSI-related hypermutations, which is in keeping with observations in DLBCL (0.3%), even though it differs from other aggressive lymphomas (e.g., primary mediastinal B-cell lymphoma).²⁶ Upon comparative analysis of WES and targeted resequencing data, we were able to demonstrate a concordance rate of 92.0% (46/50 in 18 matched samples) of mutational calls, prompting high confidence in mutational calls derived from WES, even in non-germline-paired cases. A comprehensive description of all variants described by WES as well as panel based NGS is provided in the *Online Supplementary Tables S5 and S6*. Nevertheless, we observed a significant enrichment of non-germline matched samples in non-synonymous SNV, which prompted us to include significantly mutated genes according to the MUTSIGCV analysis, only. As an exception to this rule, we also included *MYC* mutations below the statistical significance level due to their previously established clinical and functional relevance.

Recurrent copy number alterations in double-/triple-hit high-grade B-cell lymphoma

We investigated our HGBL-DH/TH cohort for SCNA employing the CONTROL-FREEC²² algorithm in tumor-normal

Table 1. Clinical characteristics of the study group.

Characteristics	HGBL (N=47)	DHL-BCL2 (N=21)	DHL-BCL6 (N=17)	THL (N=9)
Insufficient FU, N (%)	9 (19.1%)	4 (19.0%)	2 (11.8%)	3 (33.3%)
Age in years, median (range)	71 (35–89)	73 (35–88)	72 (35–89)	66 (42–76)
Sex, N (%)				
Female	22 (46.8%)	8 (38.1%)	11 (64.7%)	3 (33.3%)
Male	25 (53.2%)	13 (61.9%)	6 (35.3%)	6 (66.7%)
R-IPI, N (%)				
0	1 (2.6%)	1 (5.9%)	-	-
1-2	13 (34.2%)	5 (29.4%)	6 (40.0%)	2 (33.3%)
>2	24 (63.2%)	11 (64.7%)	9 (60.0%)	4 (66.7%)
Stage (Ann Arbor), N (%)				
I	5 (13.2%)	2 (11.8%)	3 (20.0%)	-
II	9 (23.7%)	4 (23.5%)	3 (20.0%)	2 (33.3%)
III	5 (13.2%)	1 (5.9%)	2 (13.3%)	2 (33.3%)
IV	19 (50.0%)	10 (58.8%)	7 (46.7%)	2 (33.3%)
B-symptoms, N (%)				
Yes	20 (52.6%)	10 (58.8%)	7 (46.7%)	3 (50.0%)
No	18 (47.4%)	7 (41.2%)	8 (53.3%)	3 (50.0%)
Extranodal sites, N (%)				
0	9 (23.7%)	3 (17.6%)	4 (26.7%)	2 (33.3%)
1-2	28 (73.7%)	14 (82.4%)	10 (66.7%)	4 (66.7%)
>2	1 (2.6%)	-	1 (6.7%)	-
ECOG PS, N (%)				
0-1	20 (52.6%)	8 (47.1%)	8 (53.3%)	4 (66.7%)
≥2	18 (47.4%)	9 (52.9%)	7 (46.7%)	2 (33.3%)
LDH, N (%)				
Normal	7 (18.4%)	3 (17.6%)	3 (20.0%)	1 (16.7%)
Elevated	31 (81.6%)	14 (82.4%)	12 (80.0%)	5 (83.3%)
CNS involvement at diagnosis, N (%)				
Yes	2 (5.3%)	-	2 (13.3%)	-
No	36 (94.7%)	17 (100.0%)	13 (86.7%)	6 (100.0%)
Morphology, N (%)				
DLBCL-like	32 (68.1%)	17 (80.9%)	12 (70.6%)	3 (33.3%)
Burkitt-like	15 (31.9%)	4 (19.1%)	5 (29.4%)	6 (66.7%)
Frontline therapy regimen, N (%)				
CHOP-like	25 (65.8%)	11 (64.7%)	10 (66.7%)	4 (66.7%)
R-based	31 (81.6%)	14 (82.4%)	12 (80.0%)	5 (83.3%)
Intensified*	13 (34.2%)	7 (41.1%)	3 (20.0%)	3 (50.0%)
Less intensive**	9 (23.7%)	4 (23.5%)	4 (26.7%)	1 (16.7%)
Refusal	1 (2.6%)	-	1 (6.7%)	-

CHOP: cyclophosphamide/hydroxycarbonyl/vincristine/prednisone; CNS: central nervous system; DHL: double-hit lymphoma; DLBCL: diffuse large B-Cell Lymphoma; ECOG: Eastern cooperative oncology group; FU: follow-up; HGBL: high grade B-cell lymphoma; LDH: lactate dehydrogenase; PS: performance status; R: rituximab; R-IPI: revised International Prognostic Index; THL: triple-hit lymphoma; yrs.: years. *Intensified regimens: B-ALL, GMALL, CHOEP (additional etoposide), EPOCH.**Less intensive regimens: Bendamustin, mini-CHOP (50% dose reduction), rituximab mono.

and tumor-only mode, respectively, followed by GISTIC2.0²⁷ analysis. The analysis excluded chromosomes X and Y as well as common benign copy number variants defined by the Broad Institute's panel of normals. Upon cross-referencing our findings with genomic loci of known oncogenes, tumor-suppressors and elements of significant signaling pathways we identified recurrent copy number gains in oncogenes such as *MEF2B* and *CSF1R*, which have previously been implicated in the pathogenesis of malig-

nant lymphomas.^{28,29} Further, copy number losses in tumor suppressors like *NPM1* were recurrently identified (Figure 2A and B). No significant differences were detected for genes affected by copy number alterations between the three cytogenetically defined subgroups (Fisher exact test $P>0.05$ after Bonferroni correction for multiple testing). Common CNA, as defined by the above referenced panel of normal were encountered at the expected frequencies.^{30,31}

Significantly mutated candidate driver genes and mutational signatures

Putative candidate driver genes comprised several genes previously implicated in HGBL-DH/TH pathogenesis, such as *KMT2D*, *CREBBP* and *TP53* alongside several further mutated genes such as *CDKN2A*, *LNP1* or *SI*.¹⁴ Established mutational drivers known from other B-cell lymphoproliferative disorders (e.g., FL, DLBCL, BL) were recurrently encountered (e.g., *CCND3*, *ARID1A*) (Figures 2C and 3A).^{32,33} Following SNV and InDel evaluation with MUTSIGCV, a network propagation approach (Figure 3B and C) was employed on significantly mutated genes to delineate the functional implications of significant genetic events on neighboring genes. Additionally, we investigated MUTSIGCV genes using our HGBL-DH/TH (D/THL) cohort, the cytogenetical subgroups (BCL2, BCL6, THL), as well as cohorts of ABC-type DLBCL (n= 67),³³ germinal center B-cell like DLBCL (GCB-type DLBCL) (n=45)²² BL (n=108)³⁸ and FL (n=199)³⁸ (all retrieved via cBioPortal) and overlapping genes between the five lymphoma subtypes and the three cytogenetical subtypes of HGBL-DH/TH (Figure 3D and E). In our limited cohort, distinctions regarding subtype-specific mutational signatures were found to be marginal among *BCL2/BCL6* status or Burkitt-like *versus* non-Burkitt-like morphology. However, we found *CCND3* mutations, previously reported as driver mutations in BL pathogenesis, to be significantly enriched in HGBL-DH/TH patients with Burkitt-like morphology (9/15 vs. 3/28). This

observation hints at partially similar molecular paths of pathogenesis between BL and HGBL with Burkitt-like morphology. Further, an enrichment of mutations affecting *CREBBP* in HGBL-DH/TH patients with *BCL2* rearrangement was observed, which is well in keeping with its proposed fundamental role in FL pathogenesis. Distribution of mutations within selected, significantly mutated genes is depicted in the *Online Supplementary Figure S1*. Additional profiling of mutational signatures driving HGBL-DH/TH revealed a predominance of the SBS5 (implicated in aging, potential FFPE artifacts and tobacco exposure) signature across all subtypes alongside the emphasized occurrence of the SBS6 signature (implicated in defective DNA mismatch repair [MMR]) in patients with *BCL6* rearrangements (*Online Supplementary Figure S2*; *Online Supplementary Table S7*).

Comparative analysis of mutational landscape in double-/triple-hit high-grade B-cell lymphoma, related entities and molecular clusters in diffuse large B-cell lymphoma

Next, we sought to refine the genomic taxonomy of aggressive GC-derived BCL and to investigate the mutational commonalities and differences between HGBL-DT/TH and other related pathological entities. We subsequently selected cBioPortal cohorts from several entities for their similar or divergent features of B-cell differentiation (FL, GCB-type DLBCL and BL vs. ABC-type DLBCL). A com-

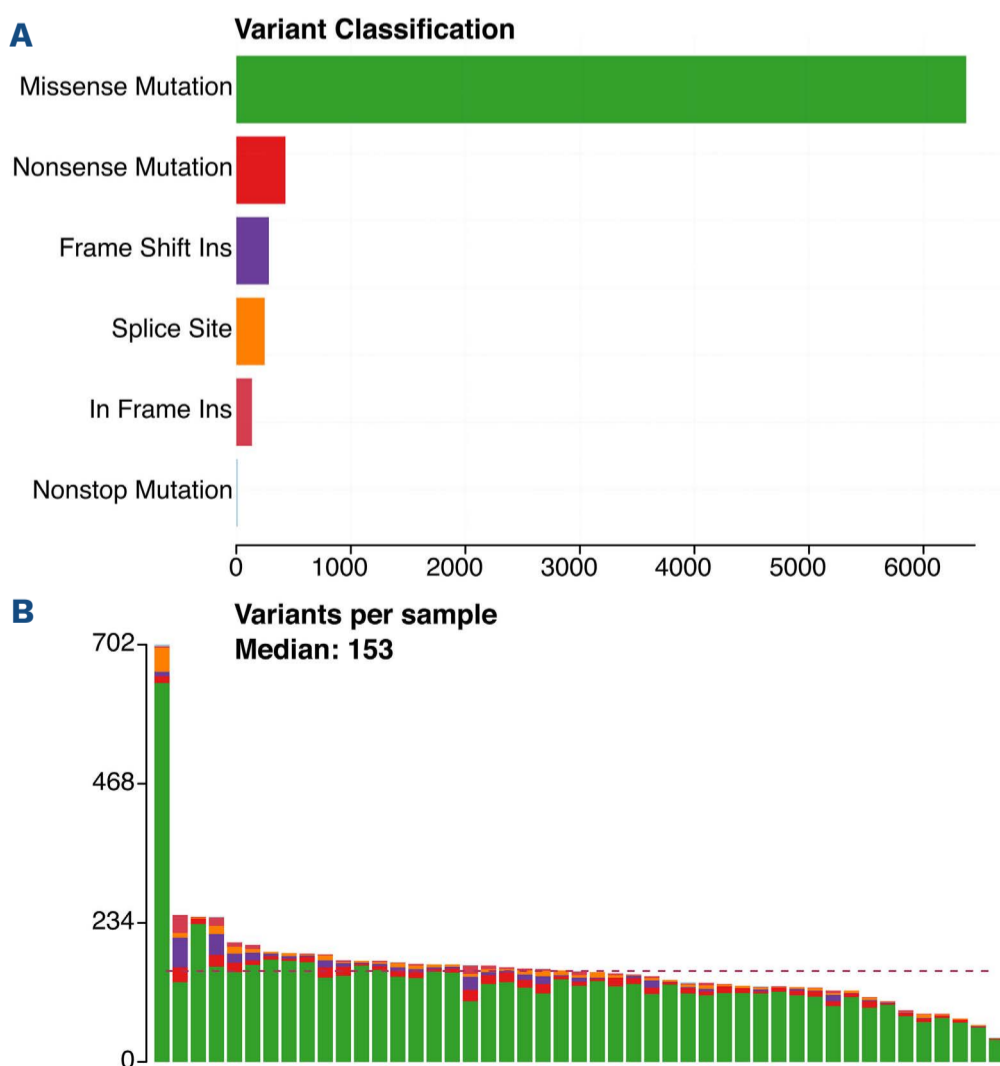


Figure 1. Variant classification and mutations per sample. Panel (A) shows the number of variants stratified by variant classification while panel (B) delineates the number of mutations per sample with a median of 153 mutations per sample. Ins: insertion.

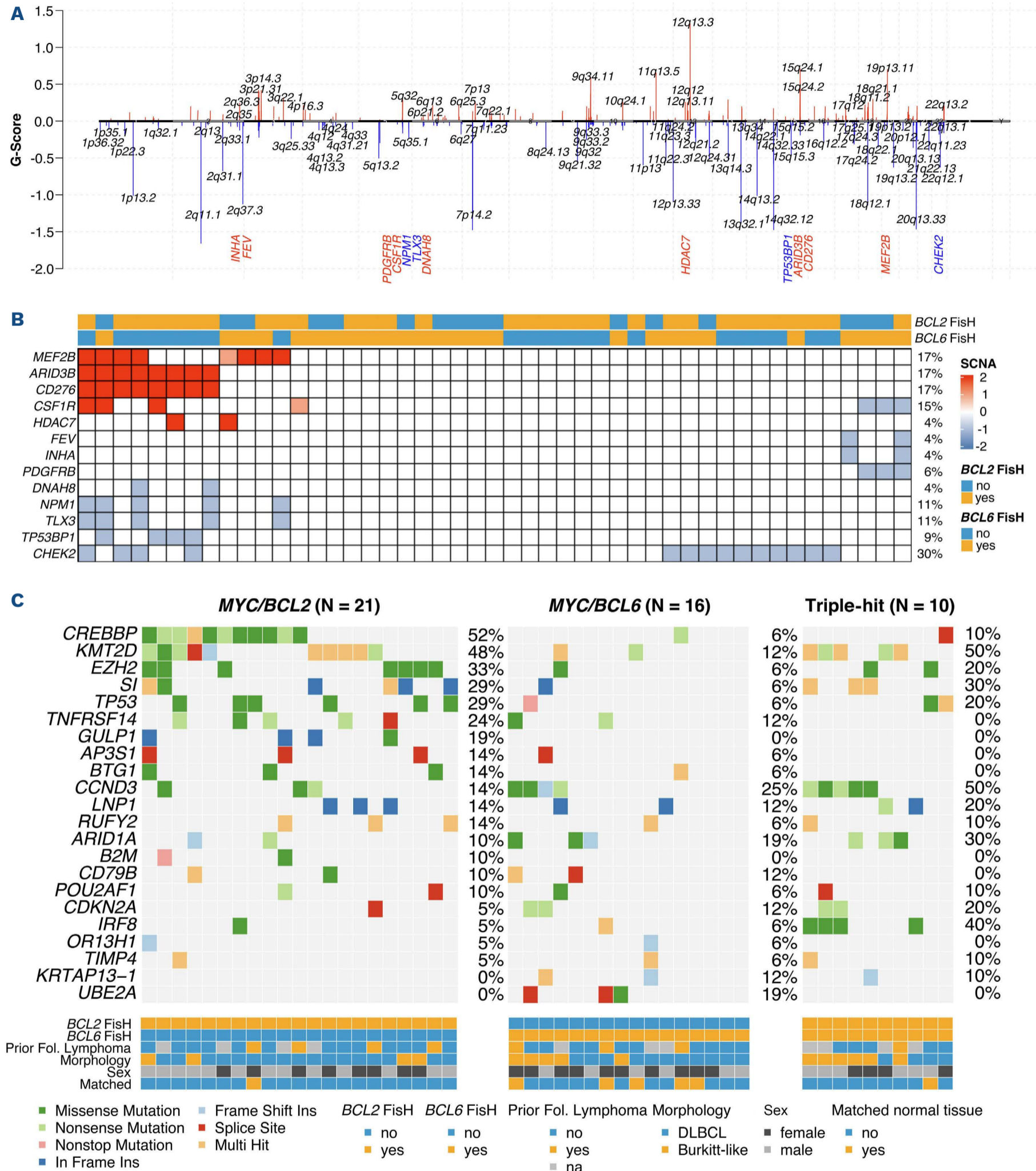


Figure 2. Genomic and mutational landscape in double-/triple-hit high-grade B-cell lymphoma. The location of somatic copy number alterations (SCNA) along the genome is shown in (A) (red bars denote gains; blue bars denote losses; gene names refer to affected oncogenes according to OncoKB). (B) Display of oncogenes from (A) and SCNA status (red refers to gain, blue refers to loss). Additionally, *BCL2* and *BCL6* status are shown for each case. Co-oncplot for genes identified as significant driver genes by MUTSIGCV ($P < 0.001$; $n = 22$) in our cohort stratified by cytogenetical subtypes is shown in (C); different types of mutations are colour coded and additional covariates are shown below the plot for each sample. DLBCL: diffuse large B-cell lymphoma; Ins: insertion; Fol: follicular.

parative analysis of candidate mutational drivers in HGBL-DH/TH (as described earlier) and cohorts of ABC-type DLCL (n=67), GCB-type DLBCL (n=45)²³, BL (n=108)³⁴ and FL (n=199)³⁴ was conducted, screening for shared as well as mutually exclusive putative driver mutations. Interestingly, we identified one overlapping candidate driver common to all entities (*KMT2D*). Additionally, *CREBBP* was found in all entities except ABC-type DLCL. Mutations affecting *EZH2*, *IRF8* and *TNFRSF14* were, however, specifically occurred in HGBL-DT/TH and FL/GCB-type DLBCL, while *CCND3* mutations appeared to be a pathogenetic feature shared between BL and HGBL-DT/TH. Additionally, *TP53* mutations posed a predominant feature of aggressive lymphomas present in all HGBL-DH/TH, GCB-type DLBCL and BL types and therefore most likely acquired during high-grade transformation (Figure 3D and E). In basic accordance with previous studies, our data suggest a common origin especially for *BCL2*-rearranged HGBL-DH/TH and FL/GCB-type DLBCL.^{14,17}

Upon comparative investigation of our current data and mutational clusters, previously described in DLBCL, we observed a striking predominance of C3/EZB cluster cases in the *BCL2*-rearranged subgroup according to the integrative molecular classification proposed by Chapuy et al. and Wright et al., respectively. This is in keeping with a significant enrichment of these cases with DLBCL morphology in terms of *MYC* rearrangement status (Figure 4; *Online Supplementary Figure S3*).^{23,24} Complementary to our analysis, employing the LymphGen algorithm (cf. *Online Supplementary Table S8*), a logistic regression indicated a significantly different number of mutated genes in C3 between the HGBL subtypes. HGBL harboring only *BCL2* were shown to exhibit the highest number of mutated C3 genes, while HGBL with *BCL6* alterations had the lowest number of mutated C3 genes (*BCL2/6* cases: $P=6.059 \times 10^{-5}$, adjusted $R^2=0.3108$). In contrast to TH cases, HGBL with *MYC* and an isolated additional *BCL6* rearrangement showed a significant decrease in the number of mutated C3 genes ($P=2.00 \times 10^{-5}$, estimate: -1.7589) (*Online Supplementary Figure S4*; *Online Supplementary Table S9*). Within the subgroup of *BCL6* rearranged cases, the BN2 cluster was more prominent than the EZB cluster. In keeping with their strong affinity towards the C3/EZB cluster, *BCL2*-rearranged cases exhibited an enrichment for mutations in *CREBBP* and *KMT2D*, while *BCL6*-rearranged cases were, in contrast, enriched for mutations in *ARID1A*. The vast majority of TH cases was also classified within the EZB cluster.

Mutational impairment of NOTCH, RTK-RAS and TP53 signaling in double-/triple-hit high-grade B-cell lymphoma

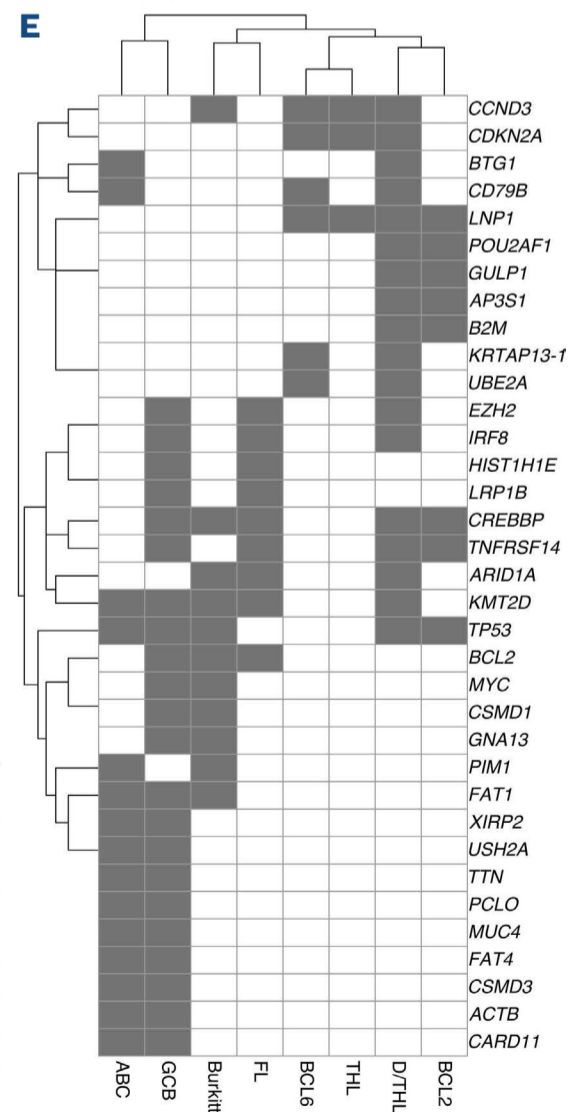
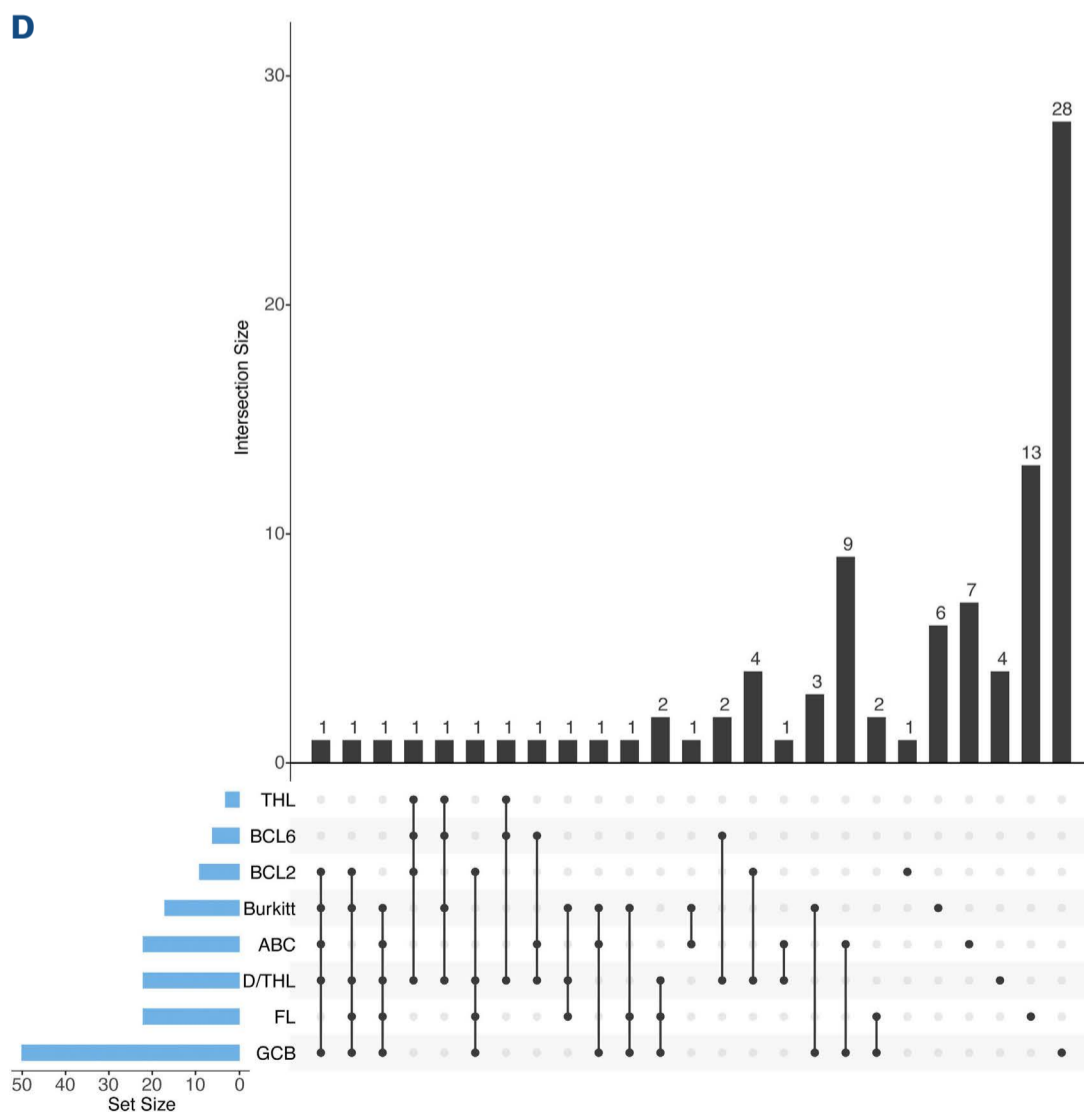
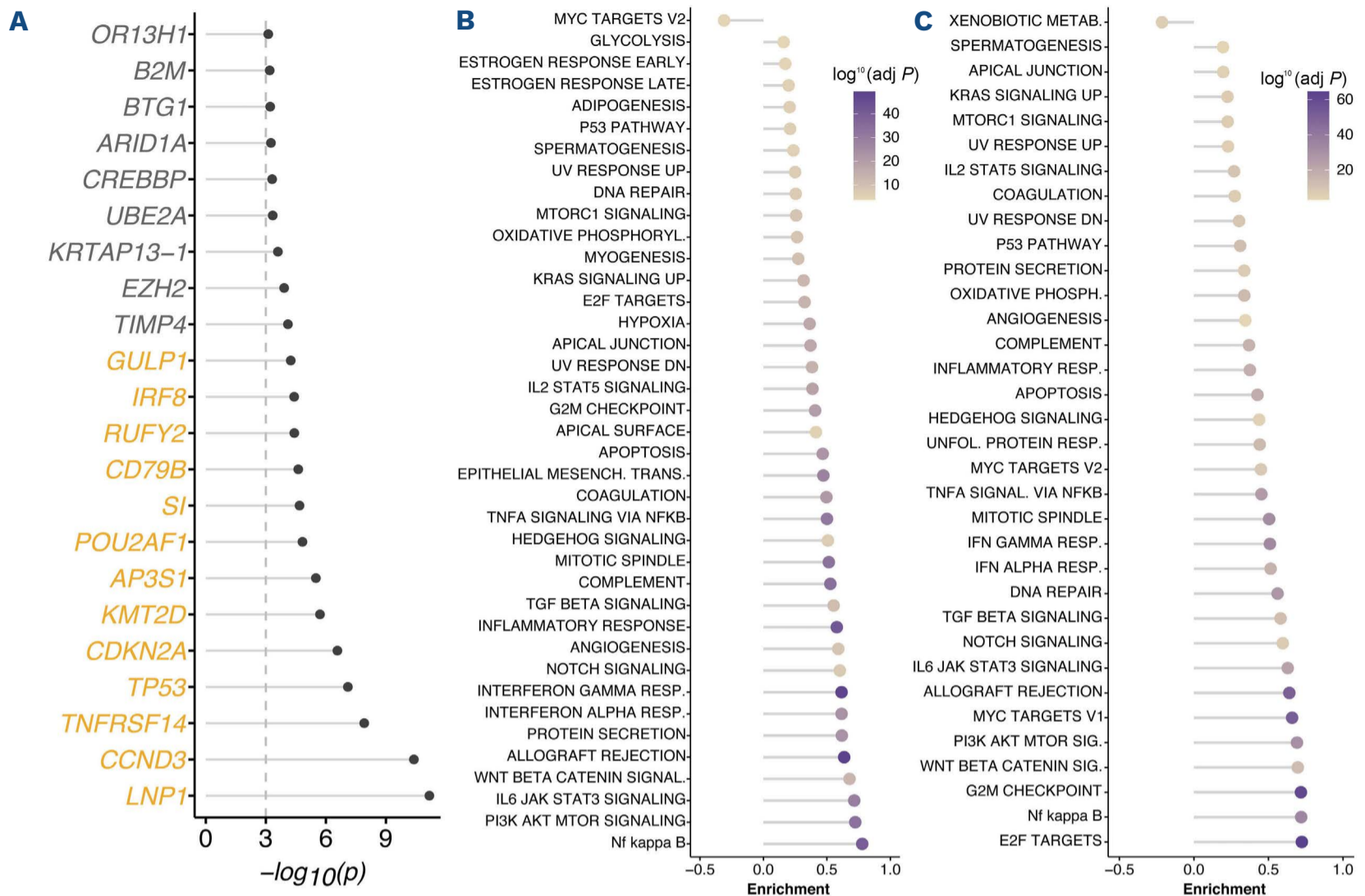
Cumulatively, we detected genetic lesions, putatively impairing NOTCH signaling in 74% of HGBL-DH/TH patients.

Expanding on previously reported *CREBBP*, *EP300* and *DTX1* mutations in HGBL we further identified recurrent mutations affecting *NCOR1* and others (*Online Supplementary Figure S5*).^{14,17} NOTCH signaling was thereby the predominant target of somatic mutation in HGBL-DH/TH, albeit with a quite heterogeneous mutational pattern affecting 35 of 47 patients with lesions in 28 of 71 genes (*Online Supplementary Figure S6A*). Most of these genomic aberrations had been previously reported to be gain-of-function mutations putatively resulting in constitutive NOTCH pathway activation in various types of predominantly GCB-type DLBCL. Several of these mutational hits including *NCOR1* and *DTX1* have been shown to herald adverse clinical outcome.^{35,36}

This remained the case when undertaking a differential downstream analysis within the cytogenetically defined subgroups (HGBL with *MYC* and *BCL2* aberrations, HGBL with *MYC* and *BCL6* aberrations and HGBL-TH), which was prompted by their significantly divergent distribution onto molecular clusters. Through this analysis a mutational signature became apparent that is additionally dominated by impairment of *TP53* and *MYC* signaling in *BCL2* rearranged cases. *BCL6* rearranged cases lacked this enrichment, while HGBL-TH cases revealed intermediate mutational features. As another recurrent feature across all subgroups we observed alterations, putatively affecting IL6/JAK/STAT signaling in 74% of patients (*Online Supplementary Figure S5*). Mutations in *PIM1* and *SOCS1* were most frequently encountered in our case series and have been previously implicated in HGBL-DH/TH pathogenesis. These genes failed, however, to reach the predefined level of statistical significance within the scope of our MUT-SIGCV analysis and required further investigation in a more comprehensive dataset.¹⁷ These candidate driver genes are supplemented by mutations in *LTB* and *STAT3* (both previously identified in HIV-associated plasmablastic lymphoma) among others.³⁷ Beyond this, we observed a relatively dispersed mutational pattern with putative driver events affecting 28 genes within the NOTCH-pathway (*Online Supplementary Figure S6A*).

In accordance with previous studies, we found mutations directly impacting NF- κ B signaling in 62% of cases (*Online Supplementary Figure S5*).³⁸ While this was, among the predominant pathways, identified through our network propagation approach, mutations affecting the pathway were narrowly detectable with only *BCL2* harboring mutations in more than three patients (34%) followed by recurrent SNV and Indels in *PARP1* (6%) and *BIRC3* (4%) and *CARD11* (4%).

The network propagation approach further underscored the mutational impairment of the aforementioned pathways alongside WNT and PI3K signaling. These observations are in accordance with preliminary impressions derived from targeted sequencing studies, employing



Continued on following page.

Figure 3. Mutational analysis for significantly mutated genes, network propagation and mutational overlap with related entities.

(A) Significance levels for significantly mutated genes in our double-/triple-hit high-grade B-cell lymphoma (HGBL-DH/TH) cohort, regardless of subgroup (MUTSIGCV $P < 0.001$; gene names in orange indicate $q < 0.1$); (B) and (C) show pathway enrichment analysis results for network propagation analysis (see the *Online Supplementary Appendix* for details) of significant MUTSIGCV genes (MUTSIGCV $P < 0.001$) for *MYC/BCL2* subgroup (*MYC/BCL2* genes included: *POU2AF1*, *HVCN1*, *B2M*, *TP53*, *AP3S1*, *LNP1*, *CREBBP*, *GULP1*, *TNFRSF14*) and *MYC/BCL6* subgroup (*MYC/BCL6* genes included: *CDKN2A*, *CD78B*, *LNP1*, *KRTAP13-1*, *UBE2A*, *CCND3*) against HALLMARK gene sets and NF κ B pathway. UpSet plot (D) showing the overlap of MUTSIGCV genes using our HGBL-DH/TH (D/THL) cohort, the cytogenetical subgroups (*BCL2*, *BCL6*, *THL*), as well as cohorts of ABC-type diffuse large B-cell lymphoma (DLBCL) ($n=67$)³⁴, germinal-center B-cell lymphoma (GCB-type DLBCL) ($n=45$)²³, Burkitt lymphoma (BL) ($n=108$)³⁴ and follicular lymphoma (FL) ($n=199$)³⁴ (all retrieved via cBioPortal); set size refers to the number of genes per cohort and intersection size shows the number of overlapping genes per comparison. Comparisons are denoted by black points and black connecting lines; (E) shows the overlapping genes between the 5 lymphoma subtypes and the 3 cytogenetical subtypes of HGBL-DH/TH; grey denotes mutated genes.

panel-based approaches.^{14,17} In addition to the divergent results from our mutational pathway analysis, we identified an enrichment of E2F targets impacted by significantly mutated genes in both DH and TH cases affected by *BCL6* rearrangements. Of further interest, we report on highly recurrent mutations in known activation-induced cytidine deaminase (AID-) and somatic hypermutation (SHM) targets such as *PIM1*, *SOCS1* and others.

Survival analysis

Following integrated analysis of molecular and clinical data we investigated genomic alterations present in >15% of patients for their impact on overall survival (OS) and progression-free survival (PFS). Hereby we identified *ARID1A* mutations to be predictive of worse clinical outcome in our cohort (OS: $P=0.0049$; PFS: $P=0.025$). Subsequent Bonferroni correction for multiple testing was performed. Thus, we identified a significant impact of mutations affecting *ARID1A* which was maintained regarding OS when correction for multiple testing was applied while its primarily significant effect on PFS was reduced to a trend of borderline statistical significance (Figure 5). A Cox proportional hazard model revealed this effect to be independent of the established clinical International Prognostic Index (IPI) prognosticators (age, lactate dehydrogenase [LDH], extra nodal manifestations, stage, and performance status; OS: $P < 0.001$; hazard ratio [HR]: 13.989; 95% confidence interval [CI]: 3.362–58.205; PFS: $P=0.001$; HR: 6.648; 95% CI: 2.098–21.061). Within the cytogenetically defined subgroups, we identified no alterations with independent impact on clinical outcome. However, a trend of borderline statistical significance towards inferior outcome in *MYC/BCL2* rearranged cases harboring *FOXO1* mutations was observed (*Online Supplementary Figure S7*).

Discussion

Here we report on WES data from an extensive cohort of HGBL-DH/TH tumors, which is to the best of our knowledge the hitherto largest cohort and most extensive molecular data set for this entity. Previous reports on

HGBL-DH/TH were limited by low sample numbers and/or targeted sequencing approaches. Contrary to this, WES here allowed to systematically define recurrent mutations, predominant mutational signatures and SCN in their respective clinicopathological context from which we report three central observations.

Firstly, being the first exome-wide mutational investigation for this rare subtype of lymphoma, we identify a significant overlap of mutational drivers between HGBL-DH/TH and FL as well as GCB-type DLBCL (e.g., *TNFRSF14*, *EZH2* and *IRF4*) as its high-grade counterpart. Aggressive transformation was associated with the acquisition of mutations in *TP53*. Moreover, shared features, including *CCND3* and *CDKN2A* mutations underscore a close molecular relation between HGBL-DH/TH and BL.^{34,39} This is additionally reflected in the enrichment of HGBL-DH/TH patients with Burkitt-like morphology for *CCND3* mutations. Further, we identify a number of significant mutational drivers not captured by previous, panel-based sequencing studies. Most frequently among these, we find *SI* mutations that have been previously implicated in CLL progression as well as mutations in *POU2AF1*, which has been recently found to be an augmented target of mutations during aggressive transformation of FL to DLBCL.^{40,41} Although *MYC* did not meet the predefined MUTSIGCV significance level in our study, we still observed mutations in 19% of cohort samples (*Online Supplementary Figure S8*), which is in agreement with previous panel-based studies.¹⁷

Secondly, upon screening the mutational landscape in HGBL-DH/TH in comparison to the molecular clusters of DLBCL, proposed by Chapuy et al. and the LymphGen algorithm proposed by Wright et al., we unveil a striking overlap of *BCL2*-rearranged cases with the C3/EZB cluster, which was previously shown to be enriched for *MYC* rearrangements and oncogenic drivers implicated in FL pathogenesis.^{23,24} We argue that a predominant subset of HGBL-DH/TH most likely corresponds to these transformed FL. This offers a potential explanation for the inferior clinical outcome of C3 DLBCL patients, despite their GCB-phenotype, through an enrichment for *MYC*-rearranged HGBL-DH/TH cases. Of note, we find the pre-

dominant impairment of *TP53* and to a lesser extent *MYC* signaling in *BCL2* rearranged cases to be in keeping with a previous study on an independent set of HGBL-DH/TH, in which we found *TP53* mutations to be a recurrent feature of HGBL-DH with *BCL2*, but not *BCL6* rearrangements.¹² Intriguingly, we further observed two

molecular subtypes in *MYC/BCL6* only rearranged cases. While selected cases were categorized within the EZB cluster, several cases revealed an association with the BN2 cluster, potentially hinting at a *MYC*-driven high-grade transformation of a precursor lesion with an origin within the marginal zone, as previously described.²⁴ In addition

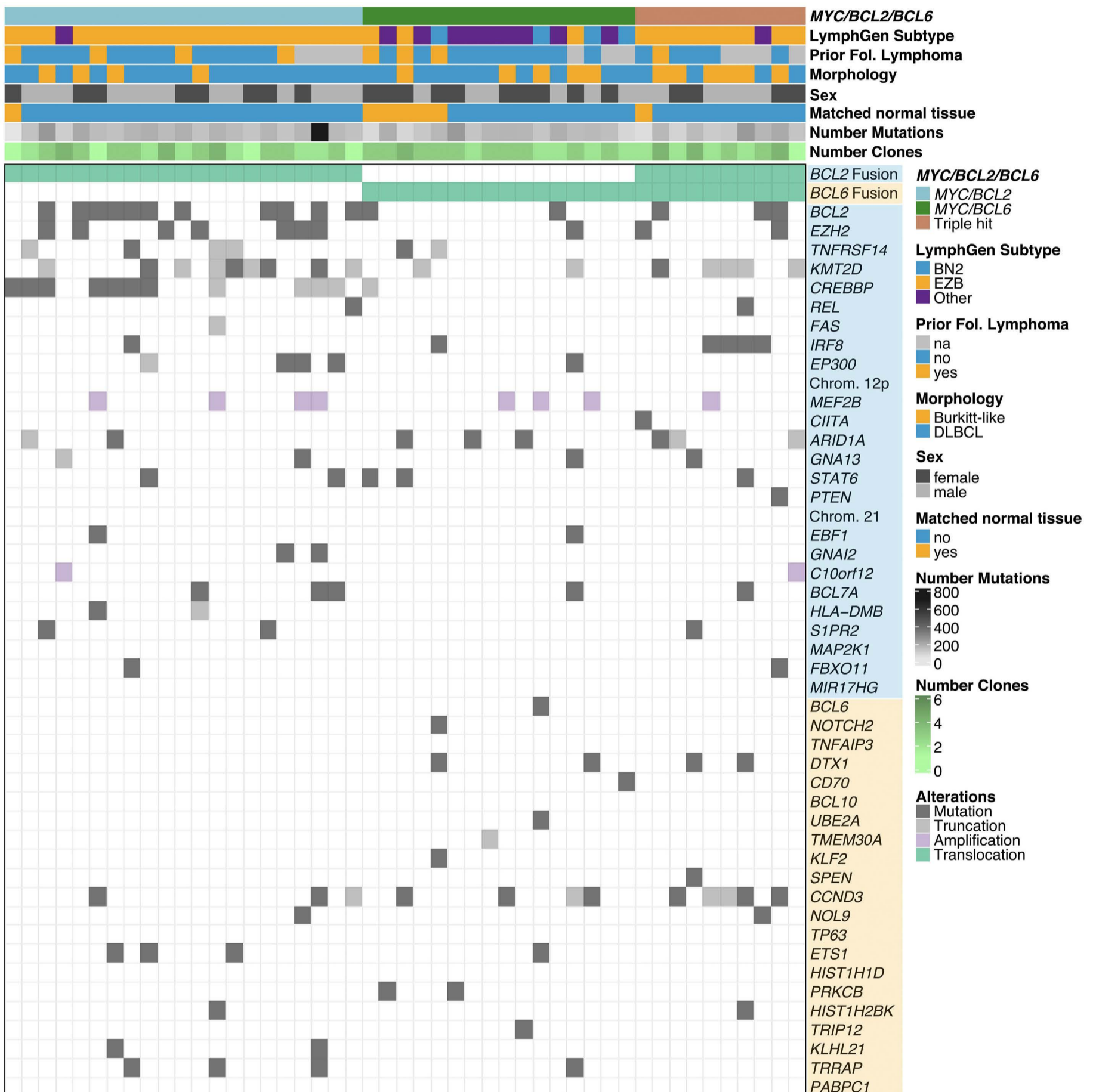


Figure 4. Allocation of double-/triple-hit high-grade B-cell lymphoma samples into the molecular subgroups/clusters of diffuse large B-cell lymphoma, according to LymphGen based on their mutational signature. Additionally, covariates are shown above the plot for each sample. Row names refer to chromosomal alterations, genes and fusions and are background coloured by their specific subtype (light blue = BN2, light orange = EZB).

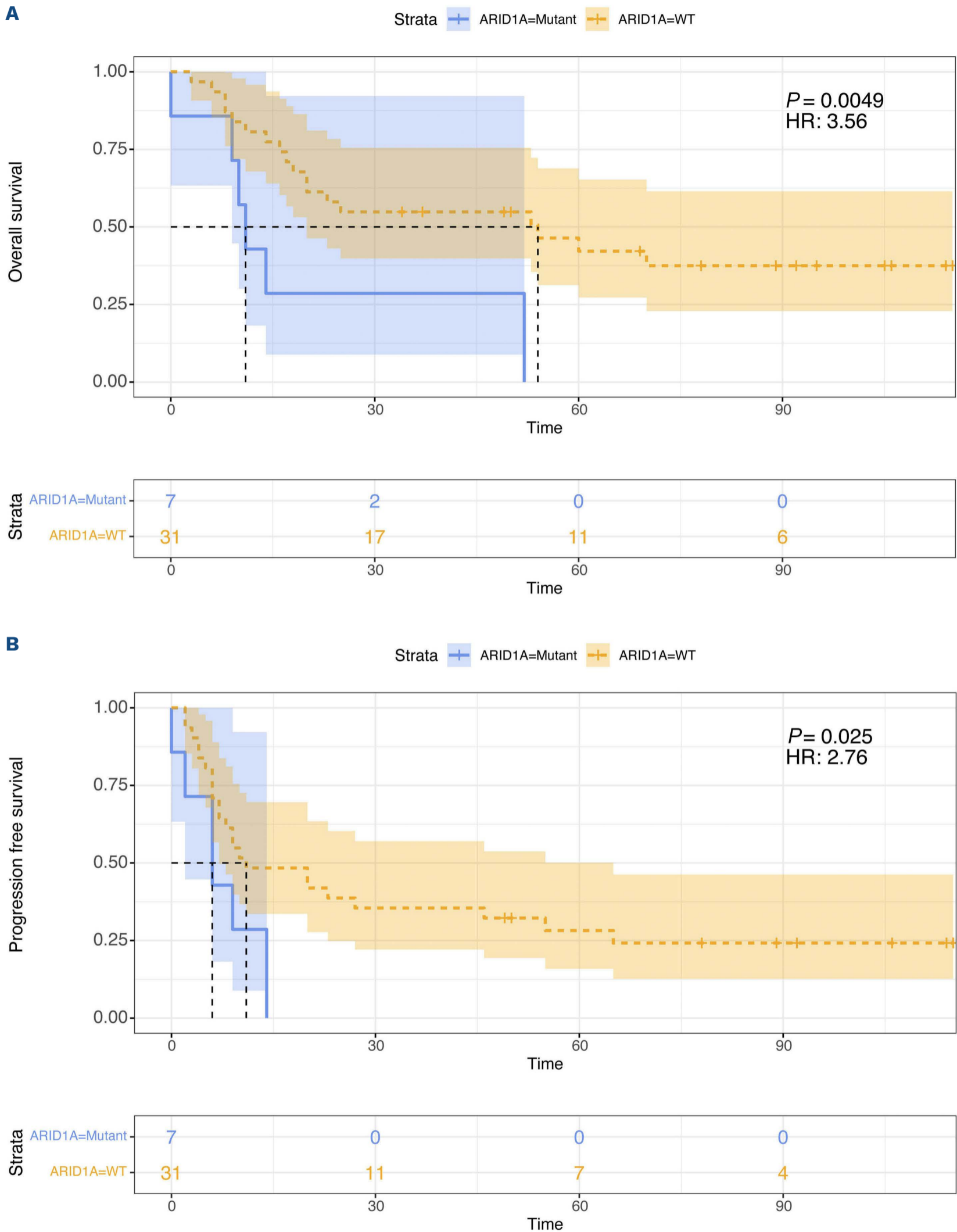


Figure 5. Survival curves according to ARID1A mutational status. (A) Overall survival (OS) and (B) progression-free survival (PFS) according to *ARID1A* mutational status. Numbers at risk alongside hazard ratios and *P*-values according to log-rank testing are provided. Subsequent Bonferroni correction for multiple testing (all genes with a mutational frequency >15% were investigated) identified a significant impact of *ARID1A* mutations regarding overall survival OS while its primarily significant effect on PFS was reduced to a trend of borderline statistical significance. Fol: follicular; DLBCL: diffuse large B-cell lymphoma.

to these observations, we found TH cases to reflect EZB lymphomas in the vast majority of cases, potentially hinting at *BCL6* rearrangements as late and non-defining events in HGBL-TH lymphomagenesis. Supporting this assumption, Pedrosa *et al.* have shown DLBCL with *BCL2* and *BCL6*, but without *MYC* rearrangements to be exclusively associated with the EZB cluster.⁴² Considering the significantly mutated genes, our observations underscore previous assumptions regarding a molecular divergence between *BCL2*- and *BCL6*-rearranged HGBL-DH.^{14,17,43} The predominant mutational distinction between these groups was the presumably FL-derived enrichment for *CREBBP* mutations in the *BCL2*-rearranged subgroup. On an exome-wide level we observed an enrichment of the SBS6 signature (implicated in defective DNA mismatch repair) and a significantly diminished congruency with the C3/EZB DLBCL cluster in the *BCL6*-rearranged subgroup. A pronounced SBS6 signature in *BCL6*-rearranged cases is in keeping with previous reports by Gu *et al.* who described genomic instability as a result of defective MMR and thereby a shorter latency to the development of *BCL6*-driven DLBCL in a murine model.⁴⁴ Of note, these findings fundamentally dispute the combined characterization in the current World Health Organization classification, despite several shared clinical aspects common to all subtypes of HGBL-DH/TH.^{1,2} Beyond *de novo* DLBCL with *BCL6* rearrangement, potential alternative explanations for this phenomenon include both clonal evolution and subsequent aggressive transformation from rare cases of *BCL6*-rearranged marginal zone lymphomas alongside *BCL2* non-rearranged/*BCL6*-rearranged FL, which were previously shown to be characterized by a heterogenous mutational landscape.^{45,46} From our data, we further deduce an intermediate role for HGBL-TH, which may indicate two divergent paths of clonal evolution originating from a *BCL2*- or a *BCL6*-driven disease with subsequent acquisition of the alternative rearrangement. The predominance of the SBS5 signature across all cytogenetic subtypes is most likely attributable to none-filtered FFPE-artifacts and advanced patient age, as was recently described.^{47,48}

Lastly, we describe a pronounced mutational impairment of NOTCH, IL6/JAK/STAT and NF κ B signaling pathways and recurrent oncogenetically relevant genes affected by SCN (including *MEF2B*, which was previously shown to be enriched in mutations/aberrations within the C3 DLBCL cluster) thereby systematically characterize the oncogenic footprint of this subgroup of lymphoma. This is further combined with the identification of novel putative mutational drivers (e.g., *NCOR1*, *DTX1*, *LTB* and *STAT3*) alongside several previously established mutational hotspots in HGBL-DH/TH. Of note, and in keeping with previous observations by Zhang *et al.*, who described an increased AID activity in DH lymphomas, we observe a sig-

nificant accumulation of mutations in known AID and SHM-targets such as *PIM1*, *SOCS1* and others.⁴⁹⁻⁵¹ Moreover, among these significantly mutated genes we describe *ARID1A* which emerges as a potential prognosticator of treatment response and outcome from our correlative assessment of clinical and molecular features of our present cohort, which was found to be independent from previously established clinical prognostic factors.

We acknowledge the shortcomings inherent to the retrospective design of the study alongside the limited availability of germline DNA for matched pair analysis. The latter aspect is reflected in a significantly elevated number of mutations in non-matched samples and an uneven distribution of controlled cases onto the cytogenetic subtypes. This prompted us to limit our subsequent analysis to significantly mutated genes (except for *MYC* and *BCL2* mutations, which were additionally included based on their proven relevance in prior studies)^{14,17,23,52} and thereby equalizing the above-mentioned effect. A minor divergence in mutational calls between WES and amplicon sequencing may be attributable to a diverse clonal architecture with mutationally different subclones as DNA samples for WES and Panel-NGS were isolated from the same biopsies but different tissue sections. Additionally, on average between 78.35% and 99.17% (first quantile 91.67%, third quantile 96.59%) of the exome targets were covered with at least 40x coverage per sample, while only variants with a minimum coverage of 40x were considered present, which might have led to the exclusion of variants on a low percentage of occasions due to too low WES sequencing coverage. However, this trade-off reduces the number of false positive variant calls and thereby enhances confidence in our calls.

Pairing of our WES-results with RNA sequencing data, preferably in an extended, clinically annotated cohort, which was beyond the scope of the present study, would further deepen our molecular understanding of HGBL-DH/TH, especially regarding cases with prominent Burkitt or Burkitt-like morphology.

In summary, our identification of distinct mutational landscapes among HGBL-DH/TH, derived from an exome-wide sequencing approach shows both overlapping and distinctive features compared with GC-derived lymphomas such as GCB-type DLBCL and low-grade FL as well as BL. Our work further underscores the developing notion of a recurrent pattern of mutational events driving a potentially unidentified preexisting FL into *MYC*-driven HGBL-DH/TH, offering insight into the molecular pathogenesis of this provisional entity. By refining the molecular taxonomy for aggressive, GC-derived B-cell lymphomas, these results call into question the current World Health Organization classification system, especially regarding the status of *MYC/BCL6*-rearranged HGBL.

Disclosure

No conflicts of interest to disclose.

Acknowledgments

AK and HB acknowledge computational support from the OMICS compute cluster at the University of Lübeck.

Funding

The research was supported by a grant to NG by the Stefan-Morsch-Foundation alongside infrastructural sup-

port. HB acknowledges funding by the Deutsche Forschungsgemeinschaft (DFG, German Research Foundation) under Germany's Excellence Strategy— EXC 22167-390884018).

Data-sharing statement

Sequencing data in bam format from WES and panel sequencing have been deposited in the European genome-phenome archive (EGA) under the accession number EGAS00001005420.

References

1. Swerdlow SH, Campo E, Harris NL, et al. WHO Classification of Tumors of Haematopoietic and Lymphoid Tissues. Vol. 2. Lyon: IARC; 2017. 586 p. ISBN: 9789283244943.
2. Rosenwald A, Bens S, Advani R, et al. Prognostic significance of MYC rearrangement and translocation partner in diffuse large B-cell lymphoma: a study by the Lunenburg Lymphoma Biomarker Consortium. *J Clin Oncol*. 2019;37(35):3359-3368.
3. Aukema SM, Kreuz M, Kohler CW, et al. Biological characterization of adult MYC-translocation-positive mature B-cell lymphomas other than molecular Burkitt lymphoma. *Haematologica*. 2014;99(4):726-735.
4. Aukema SM, Siebert R, Schuurin E, et al. Double-hit B-cell lymphomas. *Blood*. 2011;117(8):2319-2331.
5. Copie-Bergman C, Cuilliere-Dartigues P, Baia M, et al. MYC-IG rearrangements are negative predictors of survival in DLBCL patients treated with immunochemotherapy: a GELA/LYSA study. *Blood*. 2015;126(22):2466-2474.
6. Oki Y, Noorani M, Lin P, et al. Double hit lymphoma: the MD Anderson Cancer Center clinical experience. *Br J Haematol*. 2014;166(6):891-901.
7. Pedersen MO, Gang AO, Poulsen TS, et al. MYC translocation partner gene determines survival of patients with large B-cell lymphoma with MYC- or double-hit MYC/BCL2 translocations. *Eur J Haematol*. 2014;92(1):42-48.
8. Petrich AM, Nabhan C, Smith SM. MYC-associated and double-hit lymphomas: a review of pathobiology, prognosis, and therapeutic approaches. *Cancer*. 2014;120(24):3884-3895.
9. Pillai RK, Sathanoori M, Van Oss SB, Swerdlow SH. Double-hit B-cell lymphomas with BCL6 and MYC translocations are aggressive, frequently extranodal lymphomas distinct from BCL2 double-hit B-cell lymphomas. *Am J Surg Pathol*. 2013;37(3):323-332.
10. Sarkozy C, Traverse-Glehen A, Coiffier B. Double-hit and double-protein-expression lymphomas: aggressive and refractory lymphomas. *Lancet Oncol*. 2015;16(15):e555-567.
11. Wang XJ, Medeiros LJ, Lin P, et al. MYC cytogenetic status correlates with expression and has prognostic significance in patients with MYC/BCL2 protein double-positive diffuse large B-cell lymphoma. *Am J Surg Pathol*. 2015;39(9):1250-1258.
12. Gebauer N, Bernard V, Gebauer W, et al. TP53 mutations are frequent events in double-hit B-cell lymphomas with MYC and BCL2 but not MYC and BCL6 translocations. *Leuk Lymphoma*. 2015;56(1):179-185.
13. Schiefer AI, Kornauth C, Simonitsch-Klupp I, et al. Impact of single or combined genomic alterations of TP53, MYC, and BCL2 on survival of patients with diffuse large B-cell lymphomas: a retrospective cohort study. *Medicine (Baltimore)*. 2015;94(52):e2388.
14. Evrard SM, Pericart S, Grand D, et al. Targeted next generation sequencing reveals high mutation frequency of CREBBP, BCL2 and KMT2D in high-grade B-cell lymphoma with MYC and BCL2 and/or BCL6 rearrangements. *Haematologica*. 2019;104(4):e154-e157.
15. Stengel A, Kern W, Meggendorfer M, Haferlach T, Haferlach C. Detailed molecular analysis and evaluation of prognosis in cases with high grade B-cell lymphoma with MYC and BCL2 and/or BCL6 rearrangements. *Br J Haematol*. 2019;185(5):951-954.
16. Momose S, Weissbach S, Pischmarov J, et al. The diagnostic gray zone between Burkitt lymphoma and diffuse large B-cell lymphoma is also a gray zone of the mutational spectrum. *Leukemia*. 2015;29(8):1789-1791.
17. Cucco F, Barrans S, Sha C, et al. Distinct genetic changes reveal evolutionary history and heterogeneous molecular grade of DLBCL with MYC/BCL2 double-hit. *Leukemia*. 2020;34(5):1329-1341.
18. Pedersen BS, Quinlan AR. Mosdepth: quick coverage calculation for genomes and exomes. *Bioinformatics*. 2018;34(5):867-868.
19. Chen S, Zhou Y, Chen Y, Gu J. fastp: an ultra-fast all-in-one FASTQ preprocessor. *Bioinformatics*. 2018;34(17):i884-i890.
20. Li H. Aligning sequence reads, clone sequences and assembly contigs with BWA-MEM. 2013. [cited 2020 07.06.2020]. Available from: <https://arxiv.org/abs/1303.3997>.
21. McKenna A, Hanna M, Banks E, et al. The genome analysis toolkit: a MapReduce framework for analyzing next-generation DNA sequencing data. *Genome Res*. 2010;20(9):1297-1303.
22. Boeva V, Popova T, Bleakley K, et al. Control-FREEC: a tool for assessing copy number and allelic content using next-generation sequencing data. *Bioinformatics*. 2012;28(3):423-425.
23. Chapuy B, Stewart C, Dunford AJ, et al. Molecular subtypes of diffuse large B cell lymphoma are associated with distinct pathogenic mechanisms and outcomes. *Nat Med*. 2018;24(5):679-690.
24. Wright GW, Huang DW, Phelan JD, et al. A probabilistic classification tool for genetic subtypes of diffuse large B cell lymphoma with therapeutic implications. *Cancer Cell*. 2020;37(4):551-568.e14.
25. Lawrence MS, Stojanov P, Polak P, et al. Mutational heterogeneity in cancer and the search for new cancer-associated genes. *Nature*. 2013;499(7457):214-218.
26. Chapuy B, Stewart C, Dunford AJ, et al. Genomic analyses of PMBL reveal new drivers and mechanisms of sensitivity to PD-1 blockade. *Blood*. 2019;134(26):2369-2382.
27. Mermel CH, Schumacher SE, Hill B, et al. GISTIC2.0 facilitates

- sensitive and confident localization of the targets of focal somatic copy-number alteration in human cancers. *Genome Biol.* 2011;12(4):R41.
28. Brescia P, Schneider C, Holmes AB, et al. MEF2B instructs germinal center development and acts as an oncogene in B cell lymphomagenesis. *Cancer Cell.* 2018;34(3):453-465.e9.
 29. Edginton-White B, Cauchy P, Assi SA, et al. Global long terminal repeat activation participates in establishing the unique gene expression programme of classical Hodgkin lymphoma. *Leukemia.* 2019;33(6):1463-1474.
 30. Lamprecht B, Walter K, Kreher S, et al. Derepression of an endogenous long terminal repeat activates the CSF1R proto-oncogene in human lymphoma. *Nat Med.* 2010;16(5):571-9, 1p following 579.
 31. Pon JR, Wong J, Saberi S, et al. MEF2B mutations in non-Hodgkin lymphoma dysregulate cell migration by decreasing MEF2B target gene activation. *Nat Commun.* 2015;6:7953.
 32. Love C, Sun Z, Jima D, et al. The genetic landscape of mutations in Burkitt lymphoma. *Nat Genet.* 2012;44(12):1321-1325.
 33. Dunleavy K, Little RF, Wilson WH. Update on Burkitt lymphoma. *Hematol Oncol Clin North Am.* 2016;30(6):1333-1343.
 34. Ma MCJ, Tadros S, Bouska A, et al. Subtype-specific and co-occurring genetic alterations in B-cell non-Hodgkin lymphoma. *Haematologica.* 2022;107(3):690-701.
 35. Reddy A, Zhang J, Davis NS, et al. Genetic and functional drivers of diffuse large B cell lymphoma. *Cell.* 2017;171(2):481-494.e15.
 36. Meriranta L, Pasanen A, Louhimo R, et al. Deltex-1 mutations predict poor survival in diffuse large B-cell lymphoma. *Haematologica.* 2017;102(5):e195-e198.
 37. Liu Z, Filip I, Gomez K, et al. Genomic characterization of HIV-associated plasmablastic lymphoma identifies pervasive mutations in the JAK-STAT pathway. *Blood Cancer Discov.* 2020;1(1):112-125.
 38. Cinar M, Rong HR, Chineke I, et al. Genetic analysis of plasmablastic lymphomas in HIV (+) patients reveals novel driver regulators of the noncanonical NF- κ B pathway. *Blood.* 2018;132(Suppl 1):S1565.
 39. Schmitz R, Young RM, Ceribelli M, et al. Burkitt lymphoma pathogenesis and therapeutic targets from structural and functional genomics. *Nature.* 2012;490(7418):116-120.
 40. Landau DA, Tausch E, Taylor-Weiner AN, et al. Mutations driving CLL and their evolution in progression and relapse. *Nature.* 2015;526(7574):525-530.
 41. Gonzalez-Rincon J, Mendez M, Gomez S, et al. Unraveling transformation of follicular lymphoma to diffuse large B-cell lymphoma. *PLoS One.* 2019;14(2):e0212813.
 42. Pedrosa L, Fernandez-Miranda I, Perez-Callejo D, et al. Proposal and validation of a method to classify genetic subtypes of diffuse large B cell lymphoma. *Sci Rep.* 2021;11(1):1886.
 43. Clipson A, Barrans S, Zeng N, et al. The prognosis of MYC translocation positive diffuse large B-cell lymphoma depends on the second hit. *J Pathol Clin Res.* 2015;1(3):125-133.
 44. Gu X, Booth CJ, Liu Z, Strout MP. AID-associated DNA repair pathways regulate malignant transformation in a murine model of BCL6-driven diffuse large B-cell lymphoma. *Blood.* 2016;127(1):102-112.
 45. Ye H, Remstein ED, Bacon CM, et al. Chromosomal translocations involving BCL6 in MALT lymphoma. *Haematologica.* 2008;93(1):145-146.
 46. Nann D, Ramis-Zaldivar JE, Muller I, et al. Follicular lymphoma t(14;18)-negative is genetically a heterogeneous disease. *Blood Adv.* 2020;4(22):5652-5665.
 47. Petljak M, Alexandrov LB, Brummel JS, et al. Characterizing mutational signatures in human cancer cell lines reveals episodic APOBEC mutagenesis. *Cell.* 2019;176(6):1282-1294.e20.
 48. Alexandrov LB, Nik-Zainal S, Wedge DC, et al. Signatures of mutational processes in human cancer. *Nature.* 2013;500(7463):415-421.
 49. Zhang J, Shi Y, Zhao M, Hu H, Huang H. Activation-induced cytidine deaminase overexpression in double-hit lymphoma: potential target for novel anticancer therapy. *Sci Rep.* 2020;10(1):14164.
 50. Kotani A, Kakazu N, Tsuruyama T, et al. Activation-induced cytidine deaminase (AID) promotes B cell lymphomagenesis in Emu-cmyc transgenic mice. *Proc Natl Acad Sci U S A.* 2007;104(5):1616-1620.
 51. Schuhmacher B, Bein J, Rausch T, et al. JUNB, DUSP2, SGK1, SOCS1 and CREBBP are frequently mutated in T-cell/histiocyte-rich large B-cell lymphoma. *Haematologica.* 2019;104(2):330-337.
 52. Kridel R, Chan FC, Mottok A, et al. Histological transformation and progression in follicular lymphoma: a clonal evolution study. *PLoS Med.* 2016;13(12):e1002197.